Radiation of Waves by a Cylinder Submerged in the Fluid beneath an Elastic Ice Sheet with a Partially Frozen Crack

by I.V. Sturova

Lavrentyev Institute of Hydrodynamics of SB RAS, pr. Lavrentyeva 15, Novosibirsk, 630090, Russia

E-mail: *sturova@hydro.nsc.ru*

Highlights:

• Using the method of matched eigenfunction expansions for the velocity potentials, the mathematical problem is handled for solution.

• Reciprocity relations are newly found which relate the damping coefficients of the submerged body to the far-field form of the radiation potentials.

1. Introduction

Ice sheets in nature may have inhomogeneities as cracks that can be open and free or partially frozen. There are many publications on the scattering of flexural gravity waves by a straight crack. For example, review of these investigations can be found in Evans and Porter [1] and Karmakar et al. [2].

In this paper, the linear 2-D water-wave problem describing small oscillations of a horizontal cylinder is considered. The surface of a fluid is covered by two semi-infinite thin elastic plates with different properties such as density, thickness, and rigidity. The interface between floating plates is considered as a narrow straight-like crack which is parallel to the cylinder axis. In order to model varying characteristics of a partially frozen crack, two springs linking the ice sheets are introduced. The effect of a crack on hydrodynamic load of submerged cylinder is investigated.

2. Mathematical formulation

The problem is analyzed in 2-D Cartesian coordinate system with the x-axis directed along the undisturbed mean water surface perpendicular to the cylinder axis, and the y-axis pointing vertically upwards; see Fig. 1. The fluid is assumed to be inviscid and incompressible, its motion is irrotational. Two semi-infinite elastic plates Λ_1 $(x < 0)$ and Λ_2 $(x > 0)$ float on water of depth H. The plate drafts are ignored. The left plate Λ_1 is characterized by Young modulus E_1, thickness d_1, density ρ_1, Poisson's ratio ν_1; the right plate Λ_2 has, respectively, the following characteristics: E_2, d_2, ρ_2, ν_2. These plates may be connected by a vertical linear spring and a flexural rotational spring with stiffness k_{33} and k_{55}, respectively, at $x = 0$.

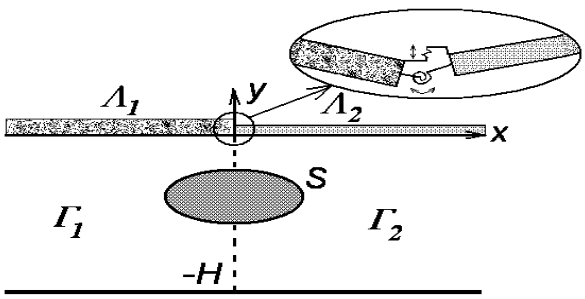

Fig.1 Schematic diagram

The wave motions are generated by the small oscillations of submerged rigid body with wetted surface S at a frequency ω with amplitudes ζ_j $(j = 1, 2, 3)$ for the sway, heave and roll problems, respectively. Under the usual assumptions of linear theory, the time-dependent velocity potential can be written as

$$\Phi(x, y, t) = \Re\left[i\omega \sum_{j=1}^{3} \zeta_j \varphi_j(x, y) \exp(i\omega t) \right]$$

where $\varphi_j(x, y)$ are complex valued functions and t is time. The radiation potentials $\varphi_j(x, y)$ satisfy the Laplace equation in the fluid domain

$$\nabla^2 \varphi_j = 0 \quad (-\infty < x < \infty,\ -H < y < 0) \tag{1}$$

except in the region occupied by the cylinder.

It is assumed that the plates Λ_1 and Λ_2 are in contact with the water at all points for all time. The upper surface boundary conditions for the fluid in contact with the plates are

$$\left(D_1\frac{\partial^4}{\partial x^4}-\omega^2 M_1+g\rho\right)\frac{\partial\varphi_j}{\partial y}-\rho\omega^2\varphi_j=0,\quad (x<0,\ y=0) \tag{2}$$

$$\left(D_2\frac{\partial^4}{\partial x^4}-\omega^2 M_2+g\rho\right)\frac{\partial\varphi_j}{\partial y}-\rho\omega^2\varphi_j=0,\quad (x>0,\ y=0) \tag{3}$$

where $D_i=E_i d_i^3/[12(1-\nu_i^2)],\ M_i=\rho_i d_i\ (i=1,2)$, g is the acceleration due to gravity, ρ is the fluid density.

The bending moment and the shear force at the connecting edge satisfy the edge conditions

$$D_1\frac{\partial^4\varphi_j(0-,0)}{\partial x^3\partial y}=-k_{33}\left[\frac{\partial\varphi_j(0+,0)}{\partial y}-\frac{\partial\varphi_j(0-,0)}{\partial y}\right],\quad D_2\frac{\partial^4\varphi_j(0+,0)}{\partial x^3\partial y}=D_1\frac{\partial^4\varphi_j(0-,0)}{\partial x^3\partial y} \tag{4}$$

$$D_1\frac{\partial^3\varphi_j(0-,0)}{\partial x^2\partial y}=k_{55}\left[\frac{\partial^2\varphi_j(0+,0)}{\partial x\partial y}-\frac{\partial^2\varphi_j(0-,0)}{\partial x\partial y}\right],\quad D_2\frac{\partial^3\varphi_j(0+,0)}{\partial x^2\partial y}=D_1\frac{\partial^3\varphi_j(0-,0)}{\partial x^2\partial y} \tag{5}$$

The edge conditions (4), (5) are the most general boundary conditions for partially frozen cracks. Taking the limit values for k_{33} and k_{55}, we can also model the free-end ($k_{33}=0,\ k_{55}=0$), hinge-connector ($k_{33}=\infty,\ k_{55}=0$) and rigidly joined plates ($k_{33}=\infty,\ k_{55}=\infty$) cases.

The boundary condition on the closed smooth contour of the submerged body S has the form:

$$\partial\varphi_j/\partial n=n_j\quad (x,y\in S) \tag{6}$$

Here, $\mathbf{n}=(n_x,n_y)$ is the inward normal to the contour S. The notations

$$n_1=n_x,\quad n_2=n_y,\quad n_3=(y-y_0)n_1-(x-x_0)n_2 \tag{7}$$

are used where $x_0,\ y_0$ are the coordinates of the center of the roll oscillations.

The boundary condition at the bottom is

$$\partial\varphi_j/\partial y=0\quad (-\infty<x<\infty,\ y=-H) \tag{8}$$

In the far field a radiation condition should be imposed that requires the radiated waves to be outgoing.

3. Method of solution

In order to solve the boundary-value problem (1)-(8), we introduce an unknown mass-source distribution $\sigma_j(x,y)$ over the contour S. We can now represent the radiation potentials at any point of the fluid in the form

$$\varphi_j(x,y)=\int_S\sigma_j(\xi,\eta)G(x,y;\xi,\eta)ds \tag{9}$$

The Green function $G(x,y;\xi,\eta)$ satisfies the following equation

$$\nabla^2 G=2\pi\delta(x-\xi)\delta(y-\eta)$$

with the boundary conditions analogous to (2)-(5), (8) and the radiation condition in the far field, and δ is the Dirac delta-function.

In order to obtain the solution for the Green function, the fluid domain is divided into two regions: the left region Γ_1 $(-\infty<x<0,\ -H<y<0)$ and the right region Γ_2 $(0<x<\infty,\ -H<y<0)$. The value of $G(x,y;\xi,\eta)$ in Γ_i is denoted by $G_i(x,y;\xi,\eta)$ $(i=1,2)$. These functions will be sought as expansions in terms of eigenfunctions of corresponding boundary value problems:

$$G_1=\alpha_1 G_0^{(1)}+R_0 e^{iq_0x}\psi_0(y)+\sum_{\substack{m=-2\\ m\neq 0}}^{\infty}R_m e^{q_m x}\psi_m(y)\quad (x<0) \tag{10}$$

$$G_2=\alpha_2 G_0^{(2)}+T_0 e^{-ip_0x}f_0(y)+\sum_{\substack{n=-2\\ n\neq 0}}^{\infty}T_n e^{-p_n x}f_n(y)\quad (x>0) \tag{11}$$

where

$$\psi_0=\cosh q_0(y+H)/\cosh q_0 H,\quad \psi_m=\cos q_m(y+H)/\cos q_m H$$

$$f_0 = \cosh p_0(y+H)/\cosh p_0 H, \quad f_n = \cos p_n(y+H)/\cos p_n H \quad (m,n = -2,-1,1,2,3,...)$$

The constants q_m's satisfy the dispersion relations

$$K_1 = q_0(1+L_1 q_0^4)\tanh q_0 H = -q_m(1+L_1 q_m^4)\tan q_m H \quad (m=-2,-1,1,2,3,...) \tag{12}$$

with $L_1 = D_1/(g\rho - \omega^2 M_1)$ and $K_1 = \rho\omega^2/(g\rho - \omega^2 M_1)$. The real positive root q_0 describes progressive wave. The roots q_{-2} and q_{-1} are complex conjugates with positive real parts, q_m's are real and positive with $(m-1)\pi/H < q_m < m\pi/H$ $(m = 1,2,3,...)$. The constants p_n's satisfy the dispersion relations similarly (12)

$$K_2 = p_0(1+L_2 p_0^4)\tanh p_0 H = -p_n(1+L_2 p_n^4)\tan p_n H \quad (n=-2,-1,1,2,3,...)$$

with $L_2 = D_2/(g\rho - \omega^2 M_2)$ and $K_2 = \rho\omega^2/(g\rho - \omega^2 M_2)$.

If the source is placed in region Γ_1 ($\xi < 0$), then the constants α_1 and α_2 are equal to $\alpha_1 = 1,\ \alpha_2 = 0$ in (10), (11). The function $G_0^{(1)}(x,y;\xi,\eta)$ is a velocity potential due to a source submerged under infinitely extended elastic plate with the properties of the plate Λ_1:

$$G_0^{(1)} = \ln\frac{r}{r_1} + pv\int_0^\infty P(y,\eta;k)\frac{\cos k(x-\xi)}{Z(k)}dk - i\pi P(y,\eta;q_0)\frac{\cos q_0(x-\xi)}{Z'(q_0)} \tag{13}$$

where pv indicates the principal-value integration, $r^2 = (x-\xi)^2 + (y-\eta)^2, \quad r_1^2 = (x-\xi)^2 + (y+\eta)^2$,

$$P = \frac{2}{k(1+e^{-2kH})}\{(k(L_1 k^4+1)[(e^{-ky}\cosh k\eta - e^{ky}\sinh k\eta)e^{-2kH} + e^{k(y+\eta)}] - 2K_1 e^{-2kH}\sinh k\eta \sinh ky\}$$

$$Z(k) = K_1 - k(1+L_1 k^4)\tanh kH, \quad Z'(q_0) \equiv dZ/dk|_{k=q_0}$$

If the source is placed in region Γ_2 ($\xi > 0$), then $\alpha_1 = 0,\ \alpha_2 = 1$ in (10), (11). The function $G_0^{(2)}(x,y;\xi,\eta)$ has the form (13) with $p_0,\ L_2,\ K_2$ in place of $q_0,\ L_1,\ K_1$, respectively.

Unknown constants $R_m,\ T_n$ to be determined to obtain the Green function completely. Because the horizontal velocity and pressure are continuous across the boundary between the regions Γ_1 and Γ_2, the full solution can be obtained from matching conditions

$$\partial G_1/\partial x|_{x=0-} = \partial G_2/\partial x|_{x=0+}, \quad G_1|_{x=0-} = G_2|_{x=0+} \quad (-H < y < 0) \tag{14}$$

Truncating the infinite series in (10), (11), the constants $R_m,\ T_n$ can be determined. The continuity conditions (14) are fulfilled in an integral sense.

Using boundary condition (6) on the body surface S, we obtain the integral equation for the functions $\sigma_j(x,y)$

$$\pi\sigma_j(x,y) - \int_S \sigma_j(\xi,\eta)\frac{\partial G}{\partial n}ds = n_j$$

Once the distribution of the singularities $\sigma_j(x,y)$ has been calculated, we can determine the radiation potentials (9).

The far-field behavior of radiation potentials φ_j has the form

$$\varphi_j(x,y) \sim C_j^- e^{iq_0 x}\psi_0(y) \quad (x\to -\infty), \quad \varphi_j(x,y) \sim C_j^+ e^{-ip_0 x} f_0(y) \quad (x \to \infty)$$

where the coefficients $C_j^\pm$ are determined from (9) using the limiting values of Green functions at $x-\xi \to \pm\infty$, respectively.

The radiation load acting on the oscillating body is determined by the force $\mathbf{F} = (F_1, F_2)$ and the moment F_3 which, without account for the hydrostatic term, have the form

$$F_k = \sum_{j=1}^{3}\zeta_j\tau_{kj} \quad (k=1,2,3), \quad \tau_{kj} = \rho\omega^2\int_S \varphi_j n_k ds = \omega^2\mu_{kj} - i\omega\lambda_{kj}$$

where μ_{kj} and λ_{kj} are the added mass and damping coefficients, respectively. There is the symmetry condition $\tau_{kj} = \tau_{jk}$. It is possible also to relate the damping coefficients to the far-field form of the radiation potentials

$$\lambda_{kj} = q_0[2D_1 q_0^4\tanh^2 q_0 H/\omega + \rho\omega Q(q_0)]C_k^-\bar{C}_j^- + p_0[2D_2 p_0^4 \tanh^2 p_0 H/\omega + \rho\omega Q(p_0)]C_k^+\bar{C}_j^+$$

where the overbar denotes complex conjugate and

$$Q(z) = \frac{1}{\cosh^2 zH}\int_{-H}^{0}\cosh^2 z(y+H)dy = \frac{1}{2\cosh^2 zH}\left(H + \frac{\sinh 2zH}{2z}\right)$$

4. Numerical results

The calculations are performed for the elliptic contour $S : (x-c)^2/a^2 + (y+h)^2/b^2 = 1$, where a and b are the major and minor axes of the ellipse, respectively, and the coordinates of its center are equal to $x = c,\ y = -h\ (h > 0)$. Rotational oscillations occur with respect to the point $x_0 = 0,\ y_0 = -h$ in (7). Input data correspond to the ice sheets Λ_1 and Λ_2 with equal properties: $E_i = 5GPa,\ \rho_i = 922.5kg/m^3,\ d_i = 2m,\ \nu_i = 0.3,\ (i = 1,2);\ \rho = 1025kg/m^3,\ b = 10m,\ a = h = 20m,\ H = 500m$. Figures 2 and 3 give dimensionless values of the diagonal coefficients of hydrodynamic load $\mu^*_{jj} = \mu_{jj}/(\pi\rho b^2),\quad \lambda^*_{jj} = \lambda_{jj}/(\pi\rho\omega b^2)\quad (j = 1,2),\quad \mu^*_{33} = \mu_{33}/(\pi\rho b^4),\quad \lambda^*_{33} = \lambda_{33}/(\pi\rho\omega b^4)$ as functions of dimensionless frequency $\omega^* = \omega\sqrt{b/g}$. Figures 2*a,b,c* and 3*a,b,c* give the hydrodynamic load for the cylinder submerged under the crack, $(c = 0)$, whereas figures 2*d,e,f* and 3*d,e,f* correspond to the position of the cylinder center in the distance $c/b = 7$ from the crack.

More detailed results for the hydrodynamic load on the cylinder and the amplitudes of the displacement of the ice sheet will be presented at the Workshop.

References

[1] Evans, D.V., Porter, R. 2003, Wave Scattering by Narrow Cracks in Ice Sheets Floating on Water of Finite Depth, *J. Fluid Mechanics*, Vol. 484, pp. 143-165.

[2] Karmakar, D., Bhattacharjee, J., Sahoo, T. 2009, Wave Interaction with Multiple Articulated Floating Elastic Plates, *J. Fluid and Structures*, Vol. 25, No. 6, pp. 1065-1078.

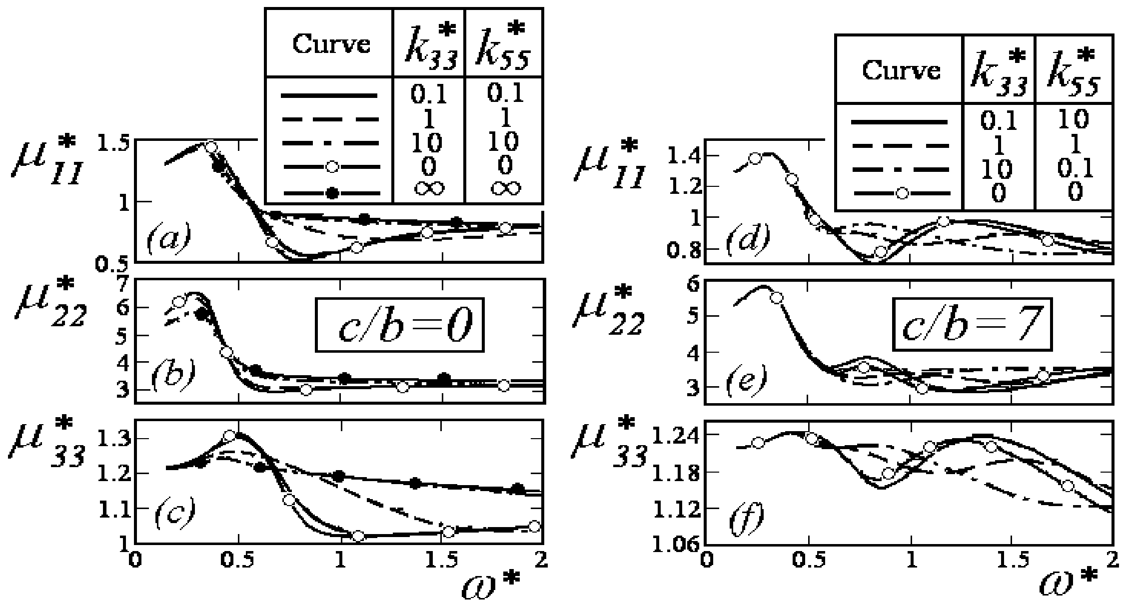

Fig.2 The added mass coefficients of a elliptic cylinder

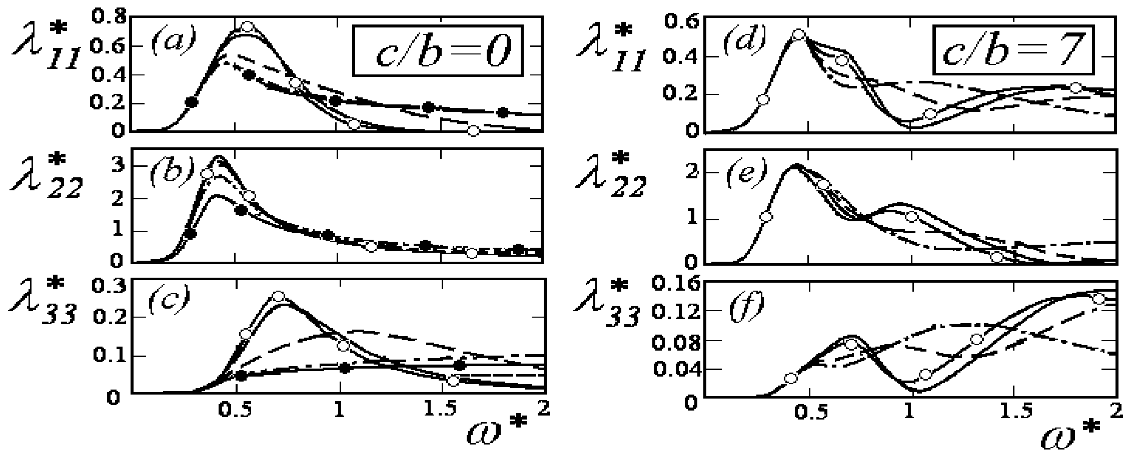

Fig.3 The damping coefficients of a elliptic cylinder